AN OPTICAL GRAVITY ANOMALY SIMULATOR

R.M.S. WHITE 1971

INTRODUCTION

The interpretation of gravity by digital methods in all but the simplest cases is a long and tedious process even with a digital computer. There is a great need for an analogue method that can easily handle complicated structures and bodies.
The main problem with gravity modelling is that the effect cannot be scaled down, so an indirect analogy was used.
The technique of simulating gravity anomalies by a light surface was originally described by Gerrard et. al. (1957).
Since the time of the original work there have been many new developments in electronic instrumentation which have enabled considerable improvements in design and operation.
The results obtained using a simple model in the simulator are compared with digital computer models of the same geometry and show good agreement.

LAMBERTS LAW ANALOGY

Surfaces that are indirectly illuminated or are glowing appear equally bright when viewed from any angle; this fact is known as Lamberts Law. The equation for the illumination at a point above such a surface and the equation for the vertical component of gravity appear in a certain form to be similar. The illumination at point 0 in Fig. 1 can be obtained by integrating over the surface.

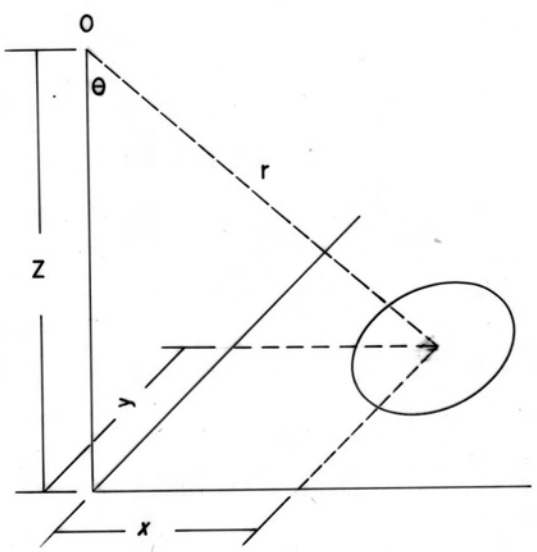

FIGURE 1.

$$L = \int_{r}^{\frac{k}{2}} \delta A_r$$

where A_r = area normal to r

if A_z is the area normal to z then

$$\delta A_r = \delta A_z \cos\theta$$

$$L = \int_{r}^{\frac{k}{2}} \delta A_z \cos\theta$$

$$= \iint_{r}^{\frac{k}{2}} \cos\theta \, dx \, dy$$

$$= \iint \frac{kz}{r^2 r} \, dx \, dy$$

$$= kz \int_{r}^{\frac{1}{3}} dx \, dy$$

Similarly it can be shown that the attraction of a mass with a density contrasts to its surrounds σ, is of a like form. The attraction at point 0 in Fig. 2 considering the effect of an element of volume dx, dy, dz at co-ordinates x, y, and z is

$$G_z = \psi \sigma \int dz \iint \frac{Z}{R^3} \, dx \, dy$$

in the vertical direction where ψ is the constant of gravitation.

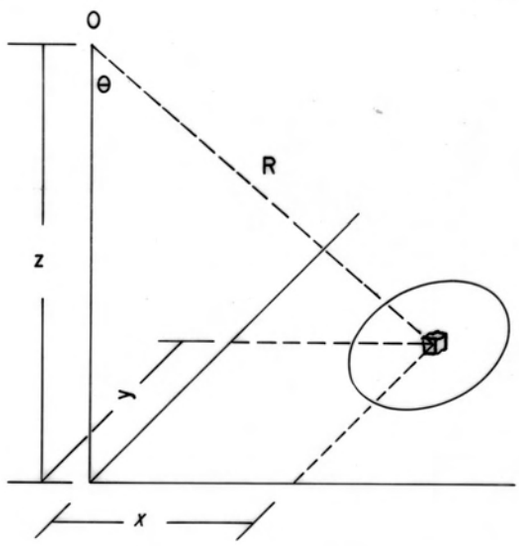

FIGURE 2.

If the body is divided into thin sections, relative to depth of burial, then the contribution of any layer to the vertical component at 0 is approximately

$$g_z = \psi \sigma \Delta z . Z \iint \frac{1}{R^3} \, dx \, dy$$

i.e. the smaller the thickness or Δz the closer is the agreement of the two equations $G_z = \Sigma g_z$ for each layer.

DESIGN OF APPARATUS

The first consideration in the design of the simulator was the size of the working area and the traverse distances. It was felt a working light area of 30 cm by 30 cm and a traverse 90 cm would be adequate, although the larger the size the greater the accuracy. It was also designed with a 90 cm maximum elevation.

The illuminated surface had to be adjustable in intensity, have a uniform illumination over the whole surface, be stable and obey Lamberts Law.

The lighting finally chosen was 8 twenty-one watt 12 volt bulbs, designed for cars. These bulbs are very stable because of their rugged construction. This gave a nominal 168 W so at twelve volts the current consumption was about 14 amps. Because a one per cent change in voltage gives about a six per cent change in light output the power supply to the bulbs would have to be very stable. One of the easiest ways to regulate the voltage is to use two twelve volt heavy duty wet cells fed by a battery charger so the same current goes in as goes out. This gives a very stable supply and the batteries do not discharge.

To control the intensity the batteries are tapped at each set of cells and a 10 amp 1.1 ohm rhestat is used for adjustment of the voltage to the lamps.

To achieve uniform illunination over the surface the bulbs were mounted in the top of a box of dimensions three feet by three feet by three feet as shown in Fig. 3. These bulbs were connected in a series parallel arrangement so they require a 24 volt supply for maximum rating.

The box is painted matt white inside which gives reasonable diffusion as well as reflection. For even greater diffusion opal perspex was used across the opening. To stop direct light there is a 10 cm lip as shown in Fig. 3 but this produces a

brighter area in the centre of the opening.

The final light adjustment was done by suspending a 23 cm x 23 cm sheet of translucent mapping paper 7 cm below the opal glass and drawing lines on it - varying the density distribution till a more even light output resulted. This gave a working area of 24 cm x 24 cm that was uniform in brightness to 1% - even better if smaller areas were used.

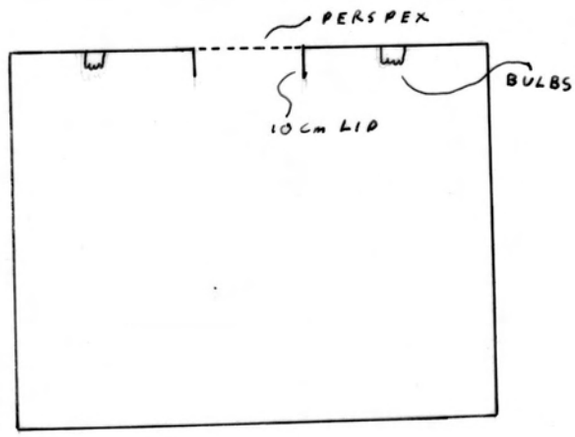

CROSS SECTION THROUGH BOX SHOWING POSITION OF LIGHTS

FIG. 3.

The degree to which the surface obeyed Lamberts Law can be seen on Fig. 4 and Fig. 5. Fig. 4 is the plot of theoretical value of brightness divided by the actual value plotted against the angle from the vertical. Fig. 5 is the actual value plotted against the same angle. Upto about 50^{o} the surface gives a good approximation to the law but diverges rapidly after this. The main reason for the divergence is that the detecting cell starts to look over the edge of the surface into the dark area. If the area of light were much larger compared to the cell, which was very close to the surface the curve would not deviate so quickly. Because the surface is gloss and not matt there is some refraction of light at low angles which causes loss but it is felt that by the time this occurs the loss from the previous source would be much greater so that compared to that is neglibible. There may also be loss due to polarisation at these low angles but again this is very small.

DEPARTURE OF SURFACE FROM
LAMBERTS LAW

FIG. 4

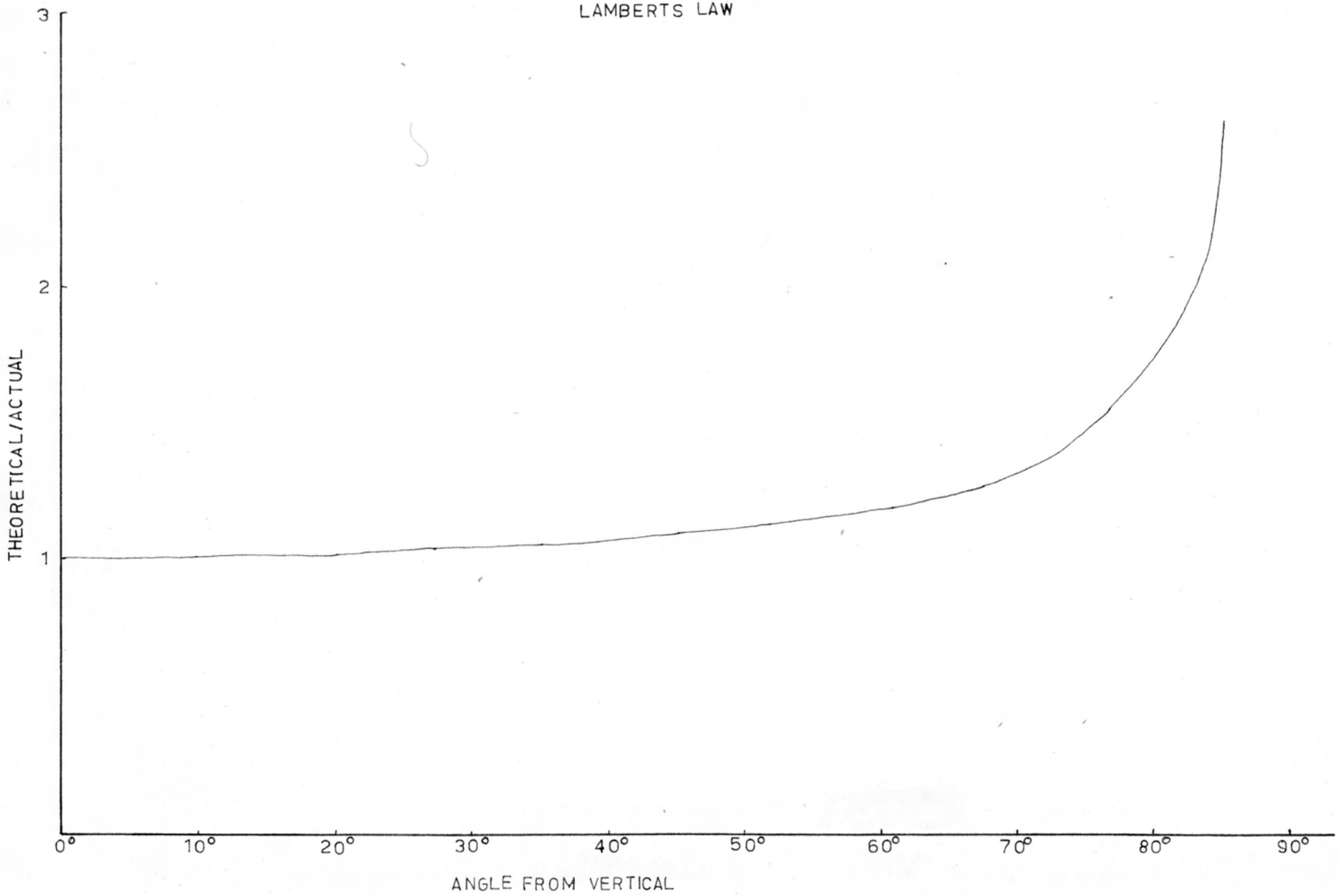

DEPARTURE OF SURFACF FROM
LAMBFRTS LAW

FIG. 5

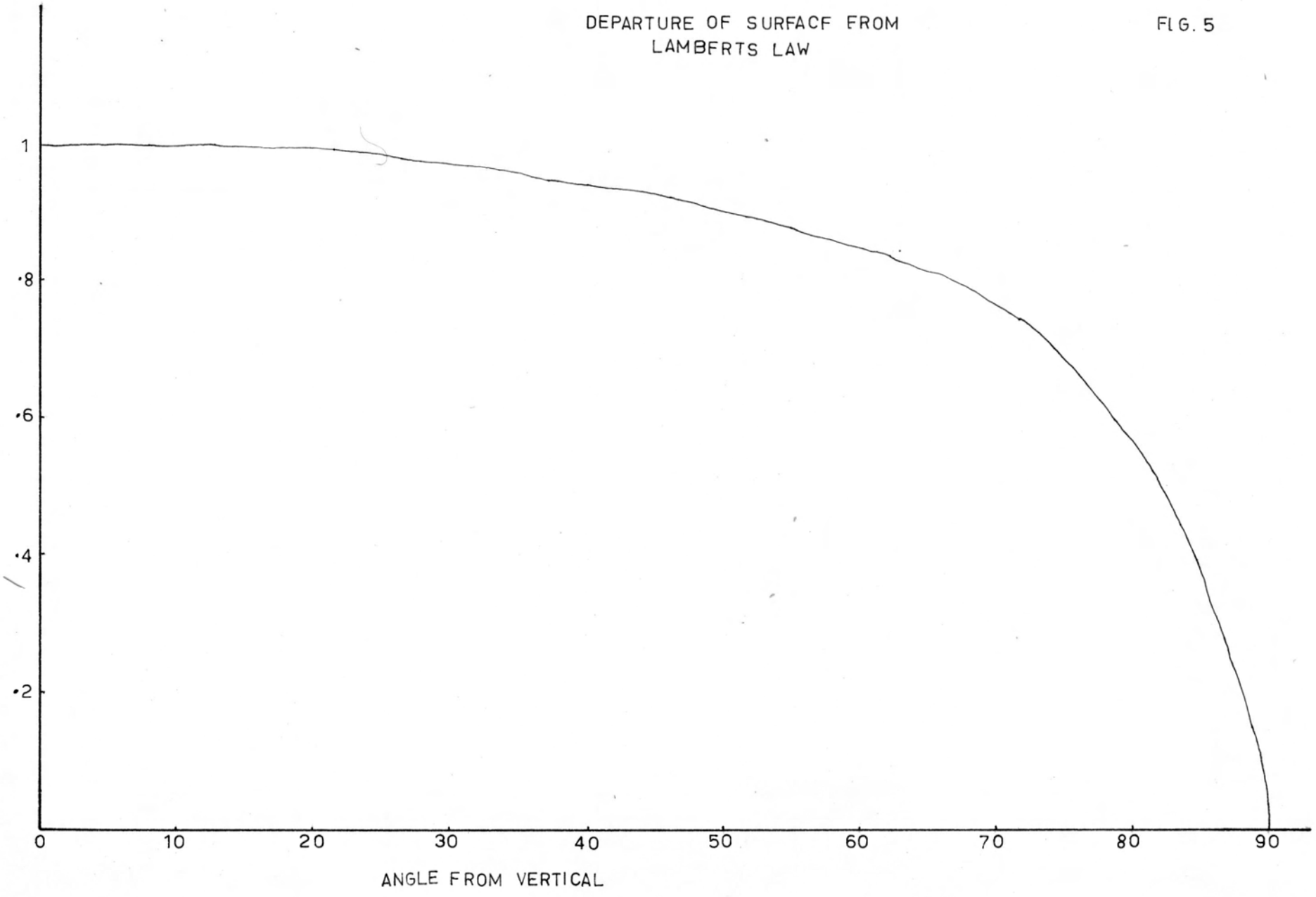

The light detector had to meet a number of specifications; the main ones being a good sensitivity over the range of light intensities being used, that the sensitive area be small and that the output be stable and preferably linear.

A number of devices were tested, the first being a cadmium sulphide photoconductive cell (ORP60). It was chosen for its small size and sensitivity, but even operated in the current mode it showed considerable non-linearity. Phototransistors suffered from an extremely small sensitive area, the base region, and so needed a lens system which gave them a very narrow field of view. Photo diodes also suffer from this disadvantage. Both devices are also fairly temperature sensitive.

A vacuum phototube (1P42) was tested, and gave a linear response but it was also temperature dependent. This device needed to be fed into a high impedance amplifier, which gave a slight temperature drift as well as noise problems. The device finally chosen was a solar cell. According to specifications, if used as a current generator and fed into a load equal to its impedance, its output would be linear. Provided the load impedance was low, the solar cell was lineary over the ranges required. The device was tested using a 1 KΩ resistor which gave a reasonable voltage output, and on testing gave a linear reponse. Fig. 6 shows the plot of output against distance from a light source which should be an inverse squared. Fig. 7 is a plot of output divided by 2 against the distance, plotted on log paper. This came out as a straight line with a slope of 2, indicating that the cell was linear. When heated the output of the cell did not change measureably until well outside the ambient temperatue ranges encountered. The output of the cell using a 2 mm aperture was about 60 mV.

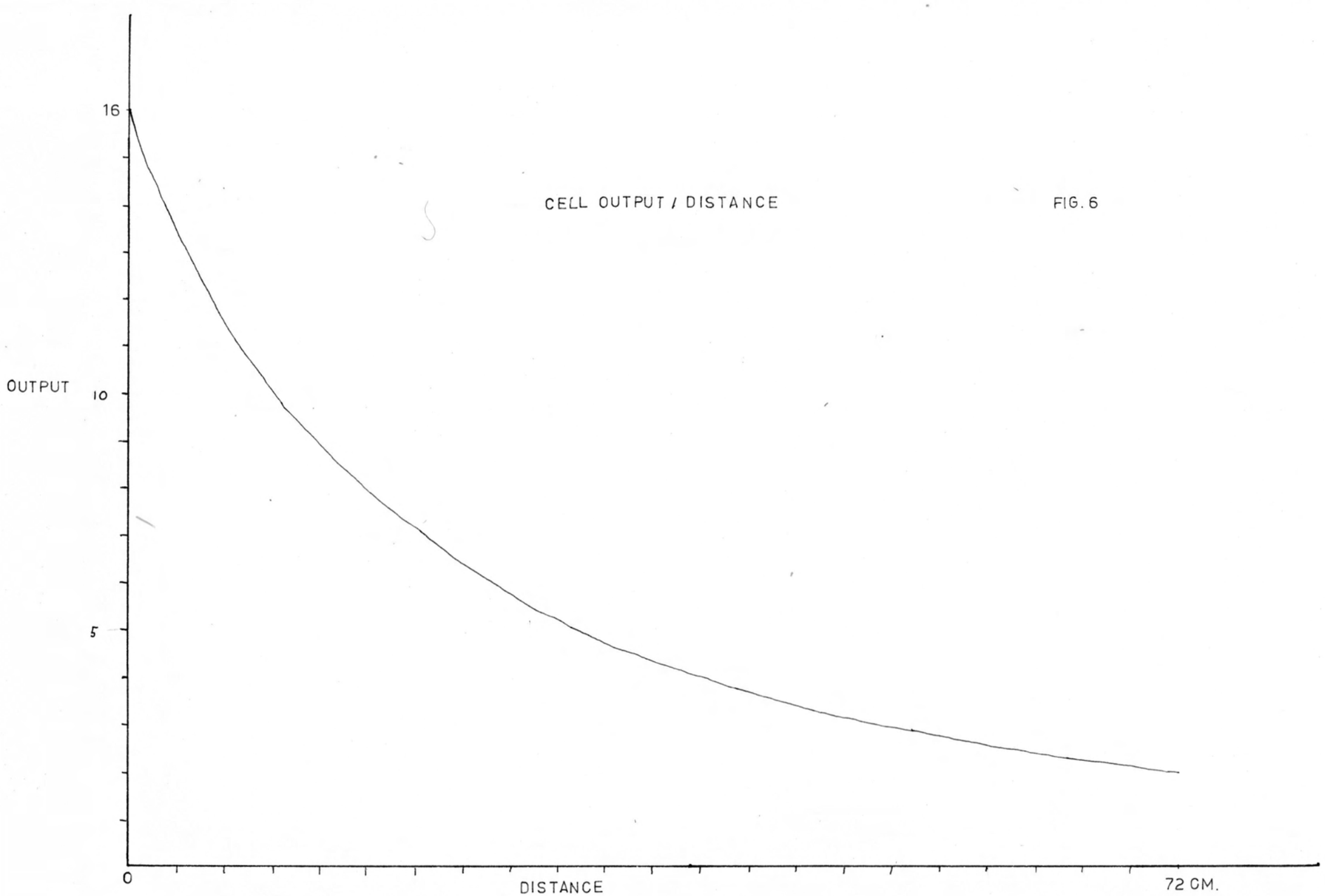

CELL OUTPUT / DISTANCE

FIG. 6

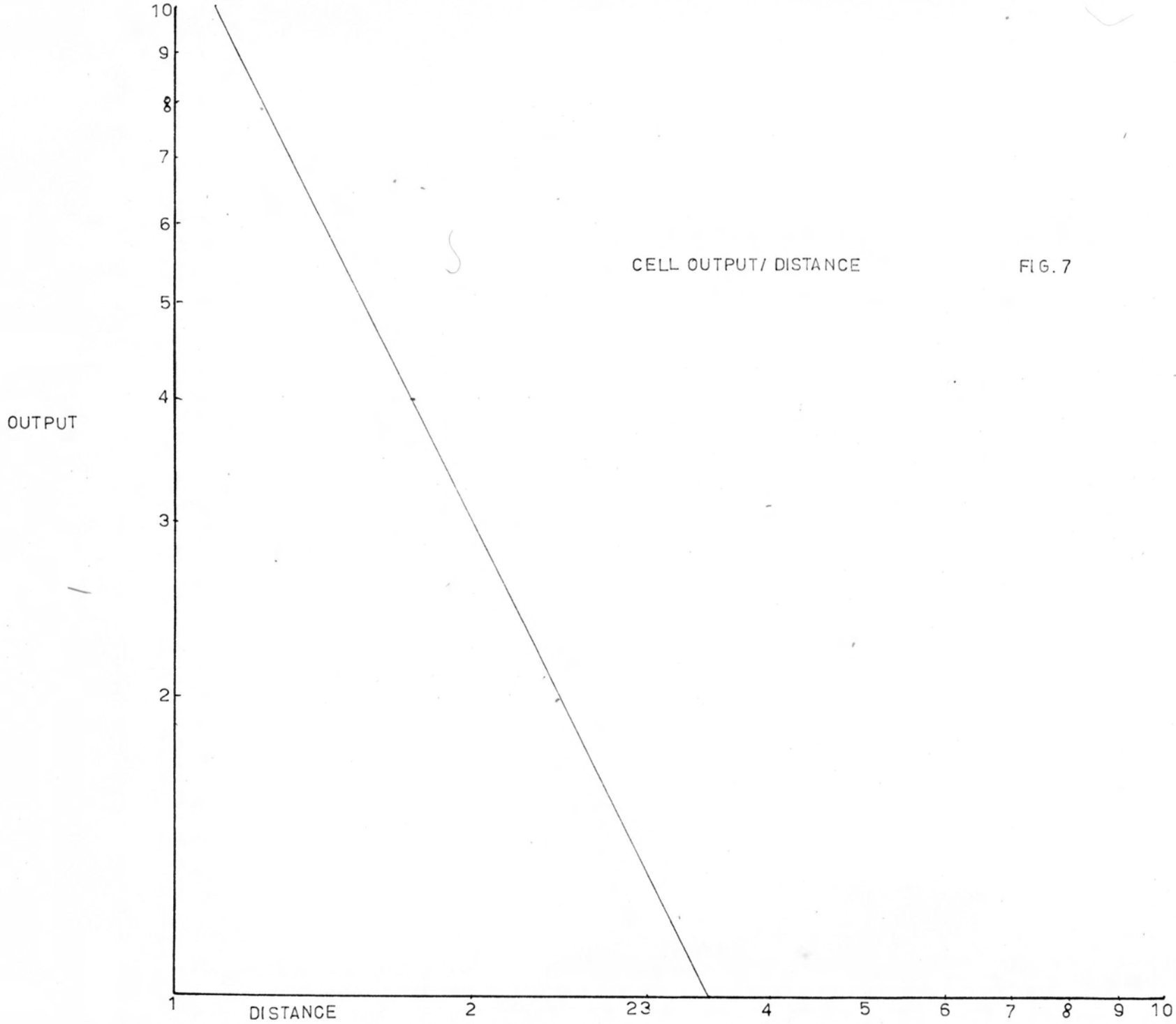

CELL OUTPUT/ DISTANCE FIG. 7

The mechanical traversing system is designed to be set at any height up to a maximum of 6m, with the cell at any position across the body. A 5 cm diameter pipe was found to be sufficiently rigid when brazed onto a plate and bolted to the surface of the box with another plate underneath. The traversing is effected by means of a threaded rotating rod and a threaded ball bushing. The rod is driven by a reversible motor, with micro-switches at each end of the rod to stop the traverse. The housing holding the arms runs on two 1.27 cm ball bushings with the threaded rod betweeen them. The arm supporting the cell is mounted in the block in two ball bushings to allow the arm to rotate. The arm is rotated by a radius arm subtended opposite the centre of the illuminated area, so that the cell always looks at this point. The arm is offset so rotation is around the centre of the cell.

A test was done with the cell to determine what effect light striking the cell at difference angles had on its output. It was found there was no difference in output 45^{o} either side of vertical. This gives a 90^{o} view for the cell that is accurate. Also the cell can be tilted so it faces the cutout when traversing off to one side of the model.

The traversing system has been fitted with a sliding potential wire so that it is possible to locate the cell when the doors of the surrounding box are closed. This also means that the output can be fed straight onto an x - y recorder. Recording eliminates the necessity of taking a large number of discrete readings,and makes graphical addition possible.

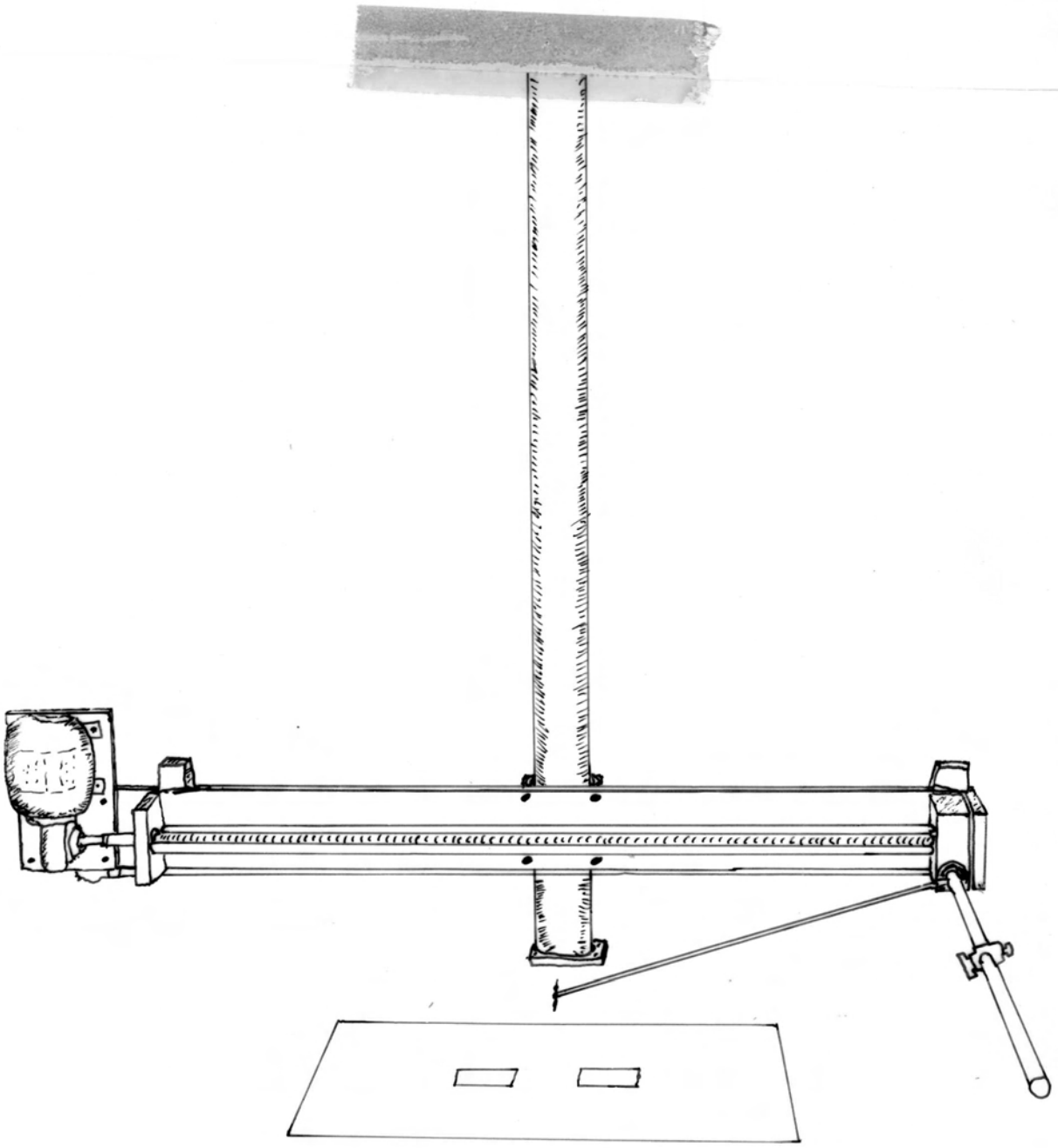

GRAVITY SIMULATOR SHOWING CLOSE UP OF THE TRAVERSING MECHANISM,MOTOR AND MICROSWITCHES.

GRAVITY SIMULATOR

READING PROCEDURE

When modelling a three dimensional body it has to be divided up into a number of horizontal sections A_1, A_2, A_3, ---A_n corresponding to depths Z_1, Z_2, Z_3, ---Z_n. The sections are drawn to a convenient scale; that chosen should enable most of the illuminated surface to be exposed as this will enhance the accuracy of the results. The principle of superposition is used and the individual effects of each two dimensional sections are summed, graphically or otherwise, to produce the total effect. The larger the number of horizontal sections used the greater will be the accuracy.

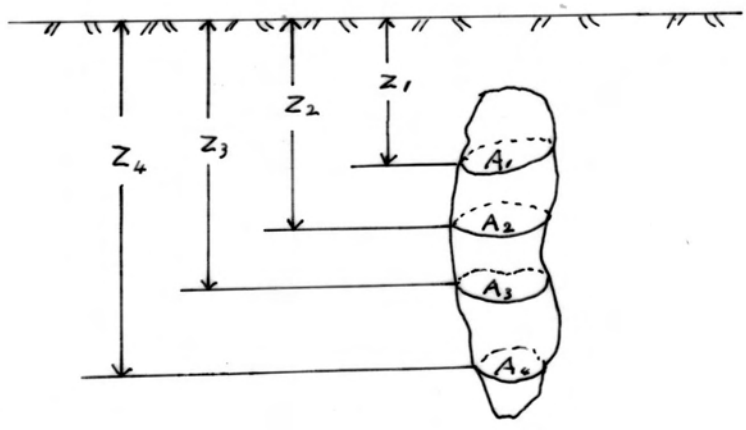

Calibration of the instrument is necessary if output requiring absolute values of milligals, rather than just profile shapes is required. This is done by centering the photocell above the illuminated surface at a height corresponding to one of the Z values to be used. The intensity of the light is set at a convenient level, and a circular cutout of 5 cm radius is inserted. The output of the cell is noted. The attraction of a circular section representating a slab of thickness 0.1 units is calculated as though it were a vertical cylinder, with a depth corresponding to Z.

$$\Delta g = 2\pi G \sigma \left[T + \sqrt{Z^2 + R^2} - \sqrt{(T + Z)^2 + R^2} \right]$$

Where Δg = the gravitational attraction

G = universal constant of gravity

σ = density contrast required for the model

t = thickness (0.1)

Z = depth to top of disc

R = Radius

The meter reading x constant (k) = Δg

Hence the calibration constant (k) = $\Delta g \quad \frac{\text{(calculated)}}{\text{meter reading}}$

Then ΔgA^1 = k x meter reading x weighting constant

$$g = \sum_{1}^{n} \Delta gA_n$$

When modelling odd shaped bodies it is easier to keep the relative thickness of the sections the same otherwise the graphical addition becomes difficult. This problem would be alleviated if digital recording were used, then, different density contrasts for different depths could readily be used, representing bodies of varying density contrasts.

ERRORS AND ACCURACY

The accuracy of the simulator can be divided up into two sections, those inherent in the mathematics and those in the mechanics of the system.

The major inaccuracy occurs when the detector is close to the surface. One reason for this is the departure of the surface from Lamberts Law. Fig. 4 shows the degree to which this surface does not obey the law, and as can be seen, up to about 50^{o} the approximation is reasonable. At shallow depths this 50^{o} will be reached more quickly and so the edges of the profile will be in greatest error. Another reason for error at small depths is caused by the limited field of view of the detector. At high body to depth ratios the detector starts to cut out part of the body as it traverses over it as shown in Fig. 8. With a field of view of 180^{o} you traverse down to a body-depth ratio of 4 before loss of light occurs. The cell has a reliable field of view of about 120^{o} with loss below 5%, so the body depth ratio can be no greater than 2 for accurate results.

Fig. 9a shows the result of too shallow a traverse over multiple bodies. The dotted line shows the approximate anomaly that should have resulted. *

Fig. 9b is the same body but with a body-depth ratio of 2. This also corresponds to the limit of detecting two subsurface bodies.

The fact that the light hitting the cell drops off with the cosine of the angle causes some small error. This is minimised by keeping the cell pointing at the cutout by means of the radius arm.

Small errors could occur due to non-linearity of the cell and amplifiers used. The cell was tested using the inverse square

* R.F. Moore's digitaly computed curves (After Nagy)

FIELD OF VIEW AND DEPTH

FIG. 8

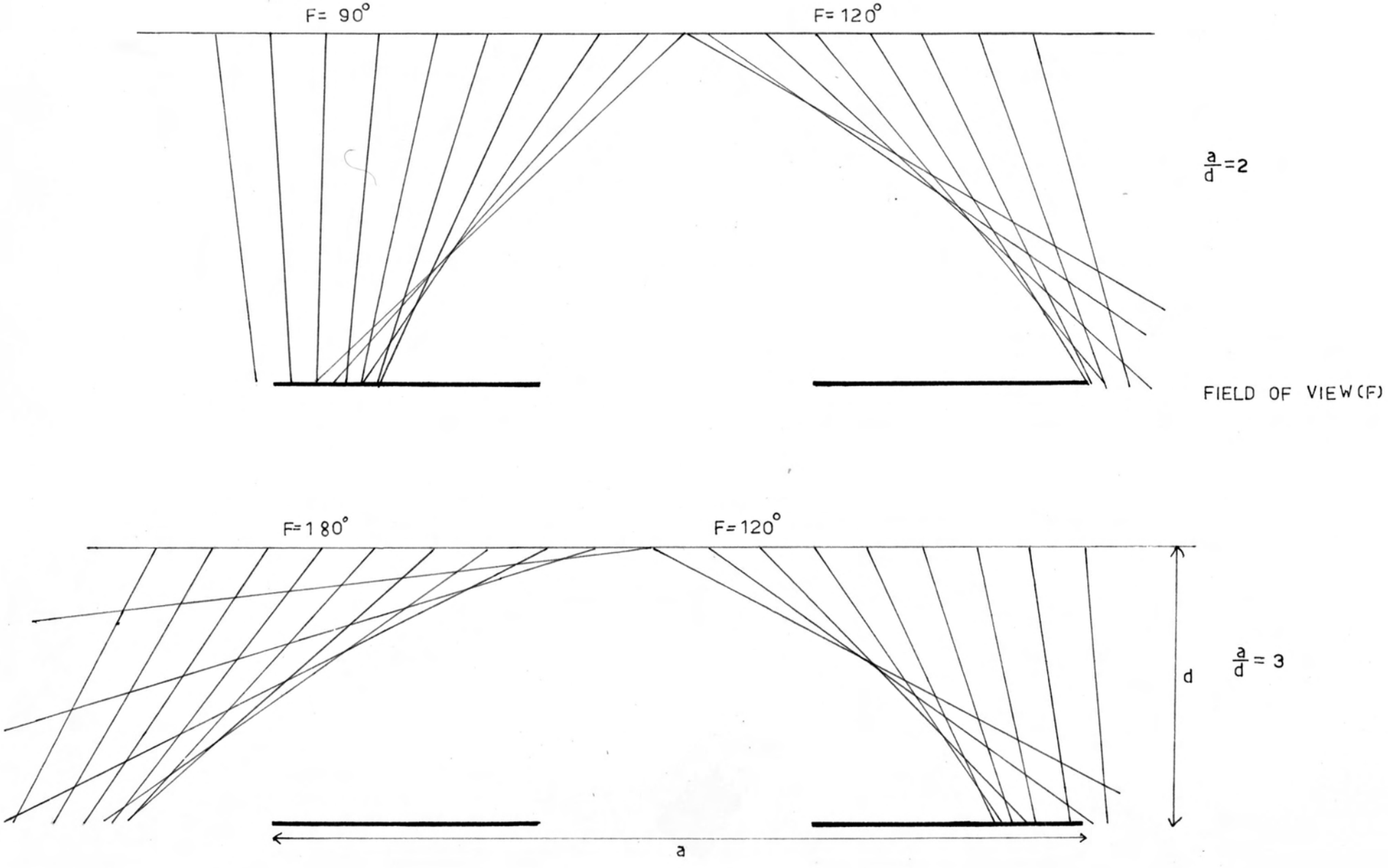

TOO SHALLOW A TRAVERSE

FIG. 9a.

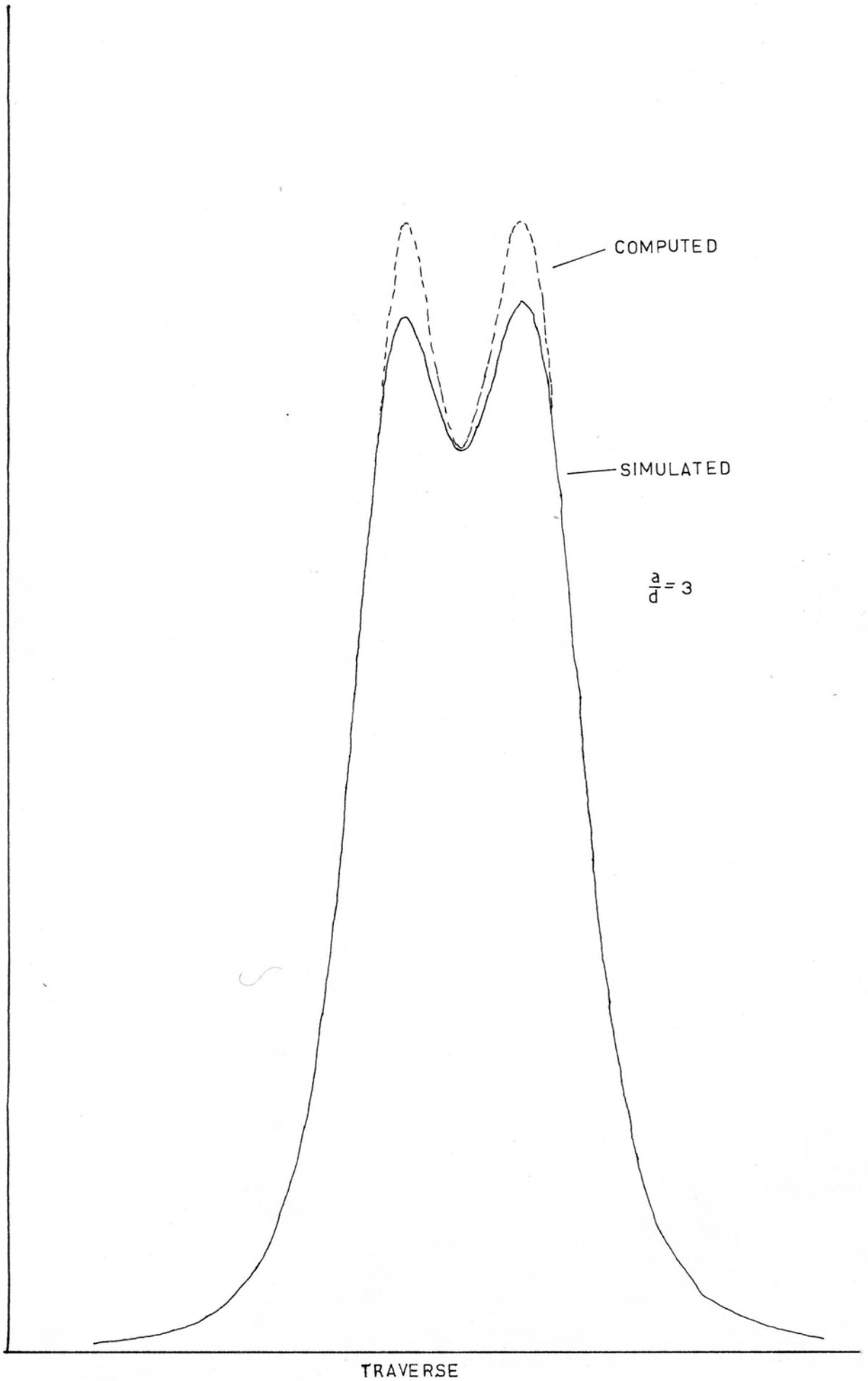

MINIMUM DEPTH SIZE
RATIO

FIG. 9 b

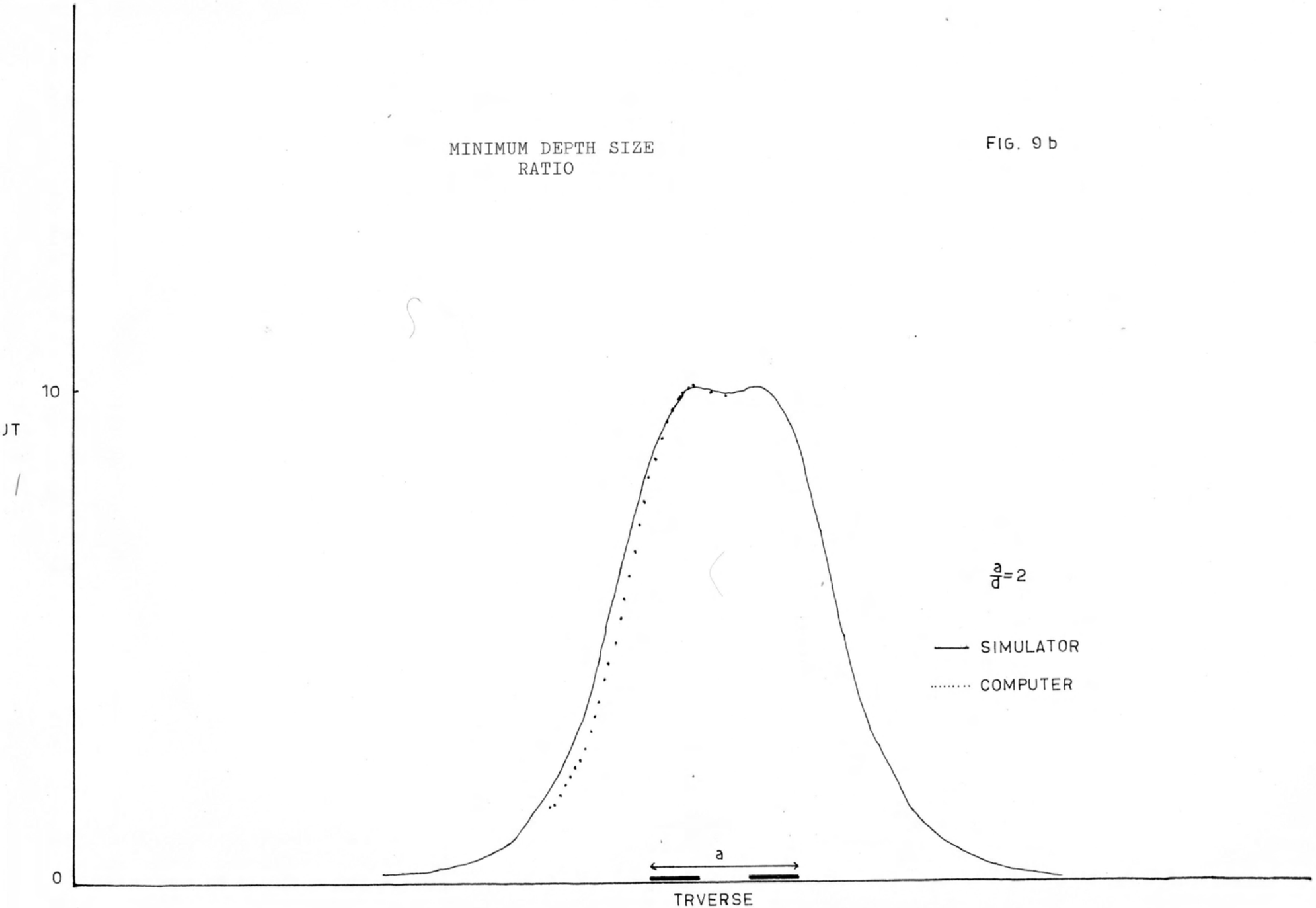

law using a point source. Because the point source was in fact of finite area the validity of the test could be questioned. At a point very close to the light the graph was not in fact linear but most testing was done at a distance which made the approximation reasonably accurate.
The other main mechanical factors are concerned with the x - y chart recorder, on which measurements were made. Because readings are repeatable in both directions and the recorder can be calibrated, errors here are small.
The last source of error is a mathematical one. As was discussed earlier the body is represented by a number of sections or layers of finite thickness while the simulator gives results for very thin slabs. The larger the number of slabs used to represent a given body the more accurate will be the result. According to Strickland et. al (1957) the error is generally less than 5% and 2 or 3% if the slice thickness is one quarter or less of the depth.
Providing the cell is about 5 cm or greater above the surface, the total error due to all these combined reasons would be less than 5%.
To improve the accuracy of results a cell with at least at 270^{o} angle of view is needed especially at low traverse heights. This would make the model far more versatile especially for a set of small widely separated bodies and near surface large bodies.

COMPARISON WITH DIGITAL MODEL

Fig.10 shows the comparison between curves done on the simulator and curves done on a digital computer. The computer used a program after Nagy (1964). The body compared was a thin square 1000m x 1000m x 1m at a depth of 1000 metres - the simulator used a 10cm x 10cm cutout with a depth of 10cm. The main source of error appears in the central region of each side and the outside edges. The error at the end of the traverse is due to the surface not obeying Lamberts Law which is seen in Fig. 5. The error in the central region is within 3% which is within the measurement errors of the simulator. A further example was done using a cube, which was approximated by dividing the cube into finite slabs. The body was 10cm x 10cm x 20cm buried to 10cm, and a profile run across the centre of the body. The depth was altered 2cm at a time and the results can be seen in Fig.11. Fig.12 shows the results of summing these graphs. The dots represent digital computerised points of the same cube with both curves normalised to their highest point. The errors are due to the approximation of thin slabs to a finite volume. This error could be cut down by using more slabs, especially at shallower depths, that is take measurements every 0.5 cm for the first few centimetres, then 1cm intervals for the next few and the very deep ones at two centimetres. Each curve would then have to be weighted differently but greater accuracy would result.

FIG. 10

COMPARISON OF SIMULATED
AND COMPUTED CURVES

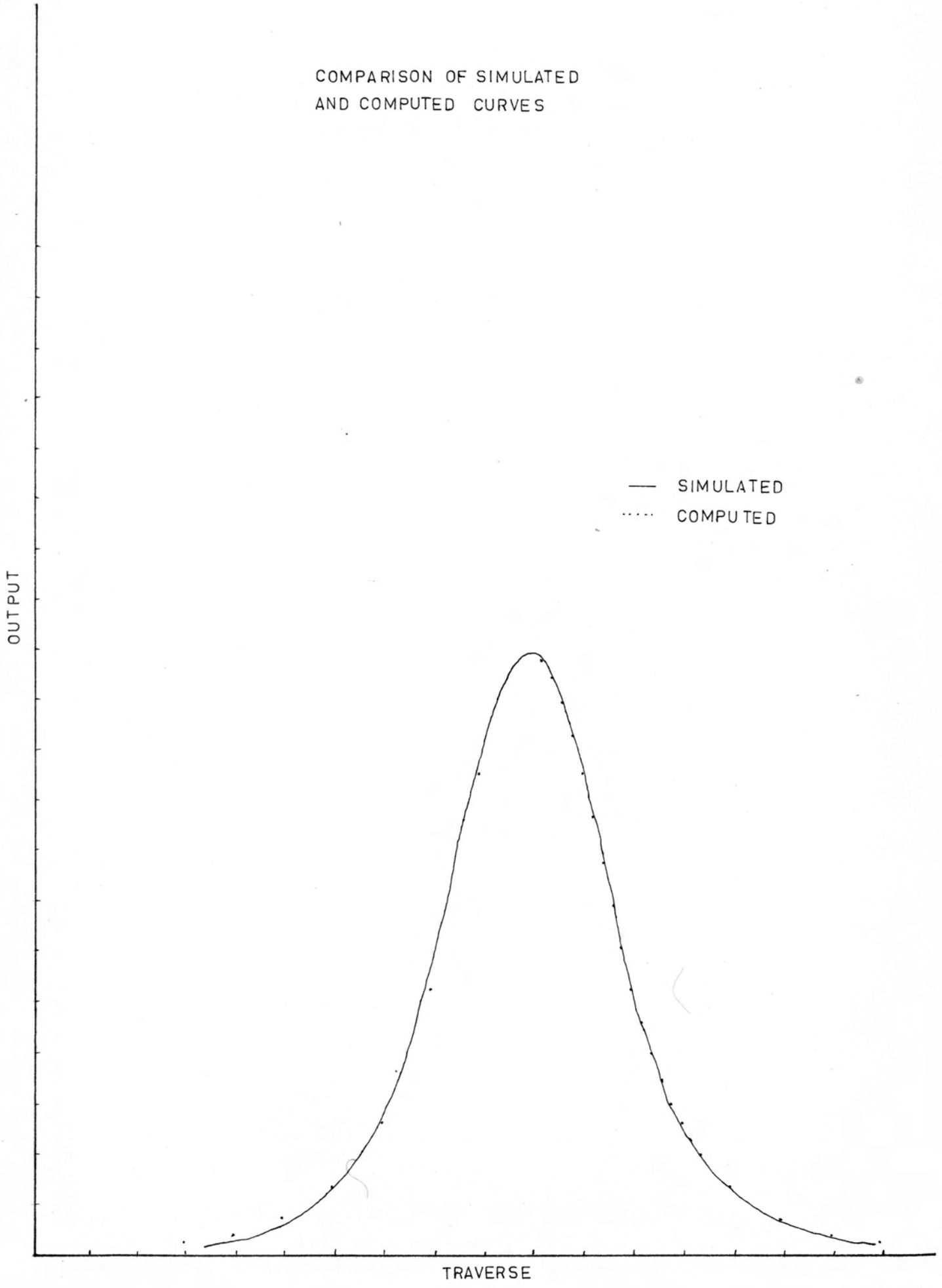

TRAVERSES AT DIFFERENT DEPTHS

FIG. 11

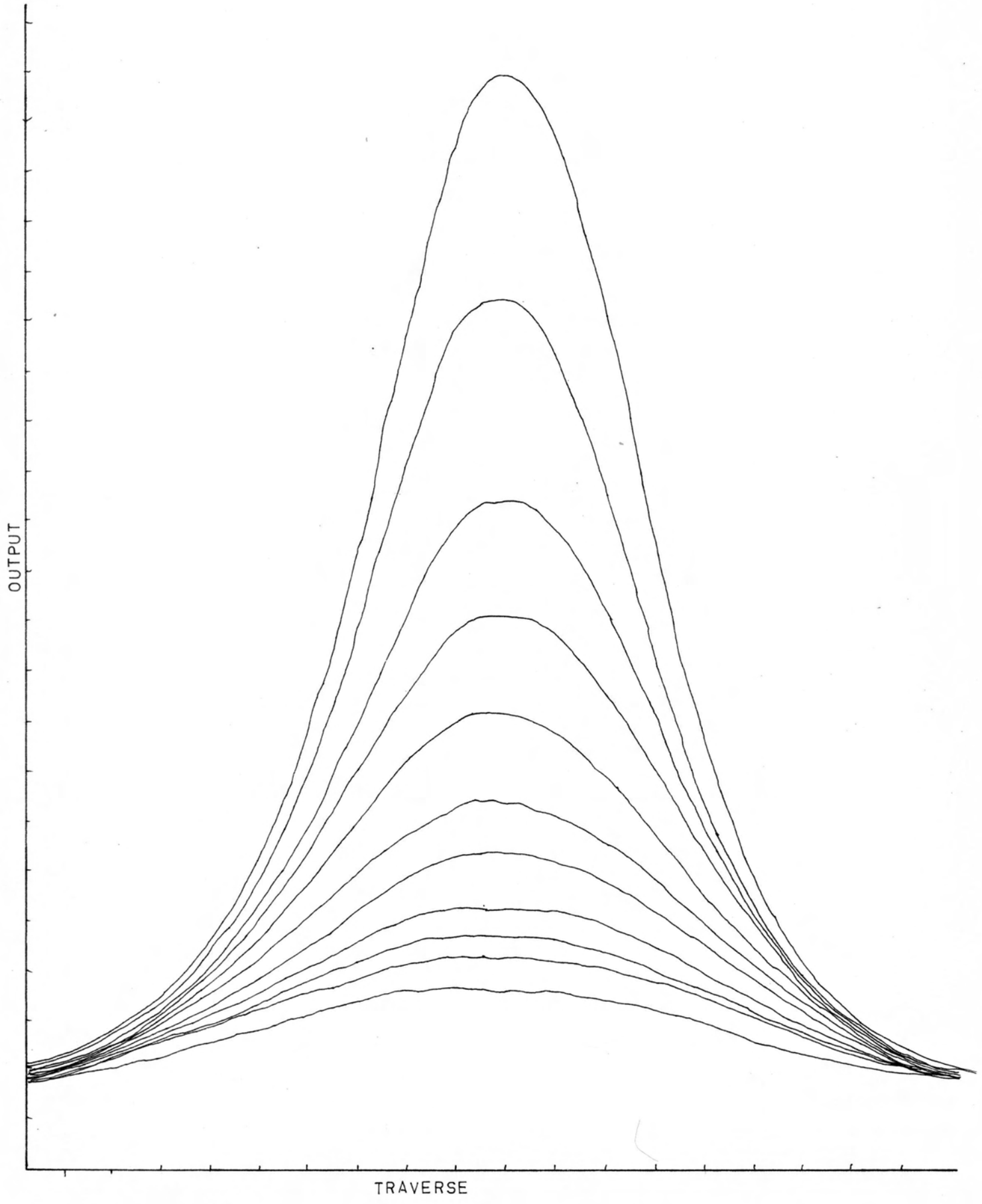

COMPARISON OF A CUBE
DIGITAL AND SIMULATED

FIG. 12

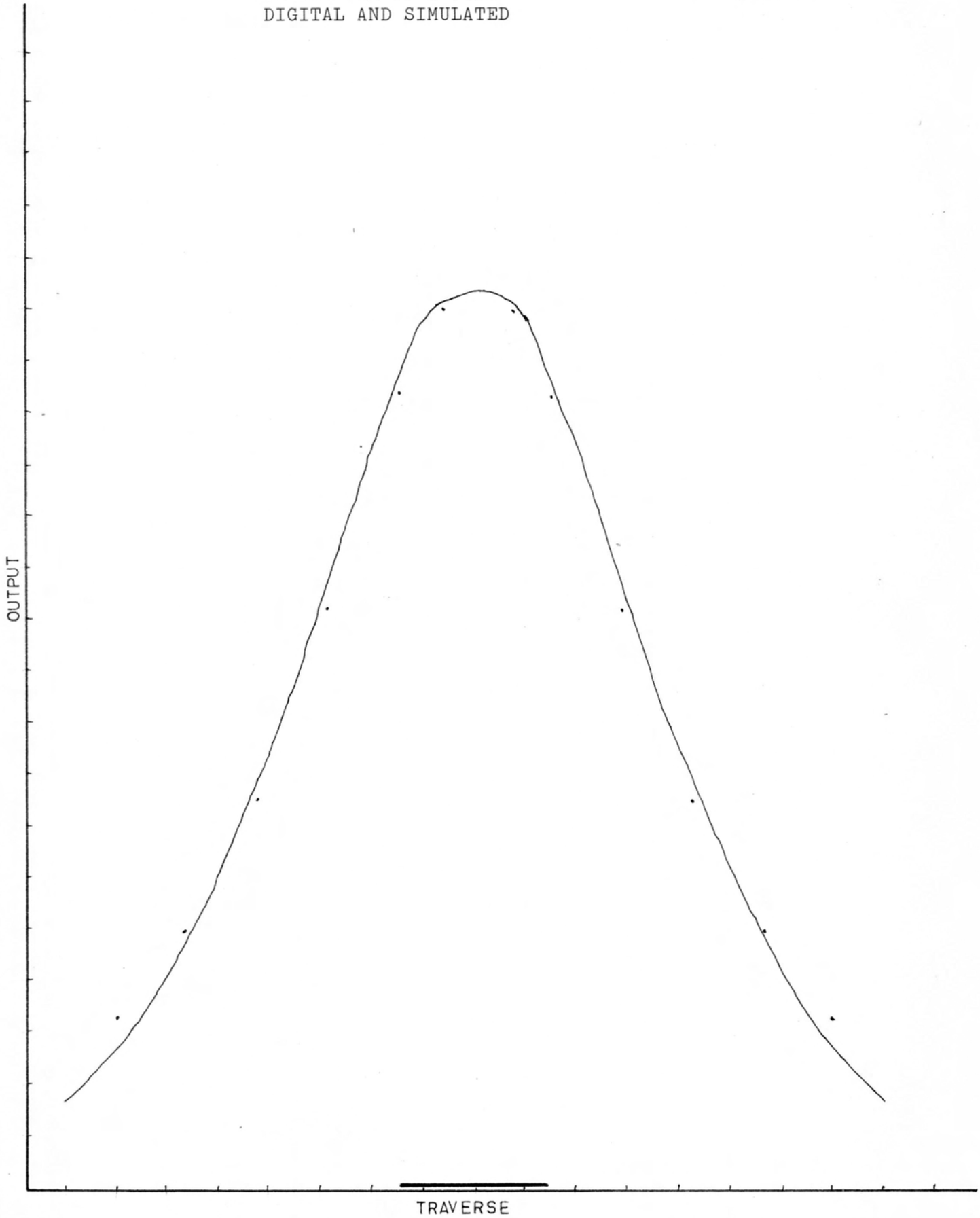

NAGY, D. (1964) "The Gravitational effect of three dimensional Bodies of Arbitrary Shape".
Department of Mines and Technical Surveys
Observatories Branch, (Unpublished Manuscript)

GERRARD, J.A.F., STRICKLAND, L., WADE, A.L., and REYNOLDS, H.K. (1957)
"Gravity Anomaly Simulator, Rev. Sc.Ins.
Vol. 28 No. 6 PP 438-442

ROY, A (1959) "Optical Analogue of Gravity and Magnetic Fields".
Geo. Prospecting 1959 Vo. 7 No. 4 PP 414-421